Fiber optic sensors for high-temperature measurements on composite tanks in fire

Aleksander Wosniok[1] · Danilo Skoczowsky[1] · Marcus Schukar[1] · Sina Pötzsch[1] · Samuel Pötschke[1] · Simone Krüger[1]

Abstract

For the purpose of increasing payload and reduce freight cost, lightweight composite tank containers used for transportation have been progressively developed during the last years. Compared to conventionally produced cylindrical steel tanks, the fiber-reinforced solutions allow greater flexibility in the tank design. Despite a number of further material-related benefits of fiber-reinforced composites as non-conductive and non-magnetic behavior as well as corrosion resistance and high strength, the optimization of their thermal degradation properties during combustion is still a challenge. To improve the fire performance of lightweight composite containers, special intumescent fire protection coatings can be applied onto the outside tank surface. This paper presents fire tests on glass-fiber-reinforced plastic transport tanks with complex geometries sheltered with different surface-applied fire protection systems. To evaluate the fire resistance of the tank structures, a fiber optic monitoring system was developed. This system is based on distributed temperature measurements using high-resolution optical backscatter reflectometry and pointwise reference measurements using fiber Bragg gratings. Thereby, all the fiber optic sensors were directly integrated in the composite layer structure of the tanks. The focus of the presented work is on the demonstration of capability of fiber optic monitoring system in such high-temperature application. Moreover, the fiber optic measurements provide new insights into the efficiency of intumescent coating applied for fire protection of fiber-reinforced plastic transport tanks.

Keywords Fire resistance · Composite material · Glass-fiber-reinforced plastic transport tank · Distributed fiber optic sensing · Optical backscatter reflectometry

1 Introduction

The still growing road transport market has opened a tough international competition. Therefore, it is becoming more and more important for the involved parties to successfully set themselves apart from other competitors in matters of cost efficiency, environmental compatibility and safety. Due to their increased corrosion and fatigue resistance as well as non-conductive properties, lightweight composite structures with their design flexibility offer a decisive market advantage of freight and maintenance cost reduction. To satisfy a fundamental requirement of high material stiffness/strength,

also the high-temperature behavior of composites must be constantly improved. Especially, the high-temperature weakening of the composite structures is still a challenge and limiting factor for further applications.

Fiber-reinforced composites typically consist of two main components, i.e., carbon or glass-fiber mats as reinforcing material and enclosing epoxy or polyester composite matrix. Although such fiber-reinforced composites have much lower thermal conductivity than metallic materials [1] used in the manufacture of traditional transport tanks, the fire resistance is directly limited by the viscous softening of the resin matrix [1, 2]. Hence, exposure to fire can result in thermal failure of composites at around 300–400 °C [3] by microbuckling and delamination between layers [4–6].

In the case of steel structures exposed to a fully developed fire, commercially available intumescent coatings [7, 8] increase the fire resistance from a few minutes to even 90 min [3]. In this paper we report about fire tests on real glass-fiber-reinforced plastic (GFRP) transport tanks to

Danilo Skoczowsky is the member of BAM till December 2017.

✉ Aleksander Wosniok
  aleksander.wosniok@bam.de

1 BAM Federal Institute for Materials Research and Testing, Unter den Eichen 87, 12205 Berlin, Germany

investigate the impact of different intumescent coatings applied onto the outside surface of the composite tanks. Apart from small structural modifications and additional usage of the fire-resistant coatings, the tanks used for tests are commercially available for transport of drinking water. The temperature distribution inside the tanks filled up to 80% with water was monitored during the fire tests using fiber optic distributed temperature sensors embedded in the layer structure of the tanks. The distributed temperature sensing (DTS) is based on a commercially available Rayleigh-based optical backscatter reflectometry (OBR). The LUNA OBR system used here allows relative temperature measurements with the spatial resolution in centimeter range. Such high spatial resolution is achieved using a coherent optical frequency-domain reflectometry (c-OFDR) [9]. The fiber optic monitoring concept is completed by the use of a fiber Bragg grating (FBG) [10] integrated in the composite layer structure [11] at the centre of the base area of each tank. Although the FBG sensor technology provides here only a pointwise temperature data acquisition, it is well proven in many other applications [12] giving a point of reference for the implemented distributed temperature sensors.

2 Fire protection concept

The study comprised fire tests on commercially available GFRP tanks for transport of water by road. The tanks were of the same design, each either coated with one of two intumescent materials (type A and B) or covered with thermoplastic foil for testing the suitability of different fire protection systems. In the reference procedure, the fire behavior of an uncoated/non-protected tank was also separately investigated. The fire tests were adapted to the requirements of the international agreements ADR/RID which regulate the European carriage of dangerous goods by road and by rail. In view of the innovative integration of fiber optic sensors (FOSs), all the test tanks can be treated as prototypes. According to the test specifications for prototype testing in accordance with paragraph 6.9.4.3.4 of ADR/RID, the GFRP transport tanks are to be filled up to 80% with water. Furthermore, the tanks have to exhibit a fire resistance of at least 30 min under fully developed fire remaining incombustible and leakproof except for drips [13, 14]. All fire tests were performed at BAM Technical Safety Test Site (BAM TTS). The test site shown in Fig. 1 was equipped with circular burners placed in the distance of 50 cm to each other consuming the total amount of 1800 kg of propane per hour [2].

2.1 Glass-fiber-reinforced plastic model tanks

The commercially available tanks tested at BAM TTS are approved for the transport of drinking water with a total
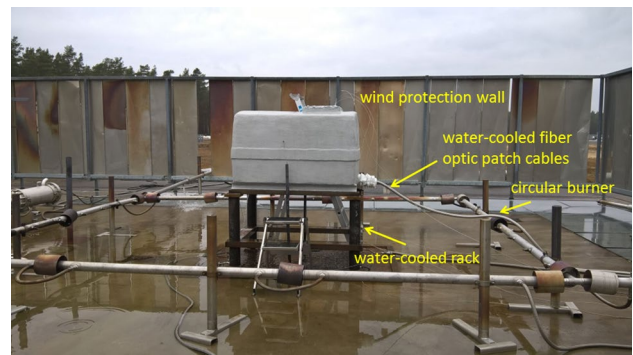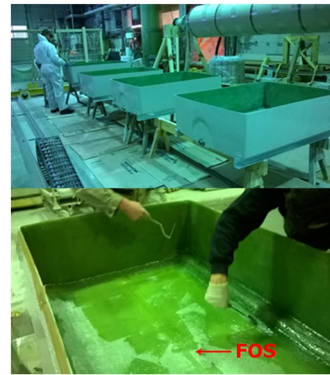

Fig. 1 GFRP tank at the test site

Layer structure bevor placing FOSs:		Thickness [mm]:
1.	gelcoat	0.2
2.	glass fiber mat type a	0.5
3.	glass fiber mat type b	0.8
4.	glass fiber mat type a	0.5
5.	glass fiber mat type a	0.5
6.	E-glass woven fabric	1.0
7.	glass fiber mat type b	0.8
8.	E-glass woven fabric	1.0
9.	glass fiber mat type b	0.8
	Total:	6.1

Layer structure covering FOSs:		Thickness [mm]:
10.	glass fiber mat type b	0.8
11.	E-glass woven fabric	1.0
12.	glass fiber mat type b	0.8

Fig. 2 Integration of FOSs in the composite layer structure of GFRP tanks. All FOSs are located in the lower shells between the 9th and 10th layer. The used two types of glass-fiber mats differ from each other in the surface weight

volume of 1.1 m^3 per tank. Following manufacture, an additional outside covering with fire protection coatings was carried out before placing at the test site as shown in Fig. 1.

To enhance comparability, all tested tanks featured the same composite layer structure shown in Fig. 2, whereas the kind of the protective coating was varied during the individual fire tests.

The layer structure of the upper shells is identical in construction to the layer structure before placing FOSs in the lower shells (see Fig. 2). The upper shells always consist of an outside gelcoat and inside 8 layers having a thickness of 6.1 cm (layers 1–9). Due to the integration of FOSs during the tank-manufacturing process, the layer construction of lower shells was extended by 3 layers, enhancing their overall thickness up to 8.7 mm (layers 1–12).

2.2 Intumescent coating

The intumescent coatings are the most common materials for passive fire protection. They insulate structures from the effects of the high temperatures and heat flux generated in

fire by formation of a voluminous foaming or swelling-insulating layer when exposed to heat. The protective effect of three following intumescent systems was investigated during the performed fire tests:

- intumescent coating of type A with an initial thickness of 9 mm increased in fire to an average of 25 mm
- gelcoat-bonded intumescent coating of type B with an initial thickness of 1 mm increased in fire to an average of 5 mm
- intumescent thermoplastic foil with an initial thickness of 2.7 mm increased in fire to an average of 50 mm.

Each individual tank was always protected with only one kind of the coatings listed above. All intumescent coatings were subsequently applied onto the outside surface of the gelcoat. Figure 3 schematically shows the cross-section of the tank wall, the distributed FOS and the intumescent coatings of both type A and type B providing best fire protection properties of the tested intumescent systems (see chapter 4).

3 Distributed fiber optic sensing method

The application-specific designed concept of distributed fiber optic temperature sensing built on the embedment of single-mode (SM) standard glass optical fibers (GOFs) in the sandwich composite structure of lower shells according to the installation plan shown in Fig. 5. The SM GOFs equipped with high-temperature-resistant polyimide coatings were thereby mechanically decoupled by putting them in thin-walled small-diameter stainless steel tubes with the
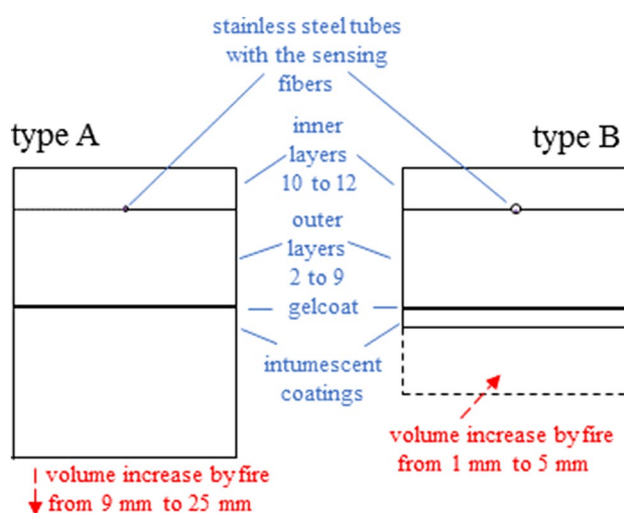

Fig. 3 True-to-size schematic showing cross-section of the tank wall with the integrated distributed FOS and the intumescent coating of type A (left) and type B (right)

wall thickness of 0.10 mm. The sensor insensibility to longitudinal strain, realized in this way, ensured pure temperature measurements performed by a commercial device based on OBR described in Sect. 3.1. The application temperatures of the applied polyimide-coated SM GOFs range from − 190 to 385 °C. The additional strain caused by differences in the thermal coefficient of expansion of the polyamide coating and the fiber material is directly included in the value of the characteristic temperature coefficients of − 1.316 °C/GHz for the OBR-based distributed sensor and 11.50 pm/ °C for the FBG sensors, respectively. These values were determined using a heating oven Heraeus T6030 in the temperature range up to 300 °C. The independent verification was carried out with a Pt100 temperature sensor based on the resistance measurement principle.

The additional FBG integration thus ensured a pointwise fiber optic reference temperature measurement. In case of composite tanks coated with type B, an additional bare wire type K thermocouple with an outer diameter of 1.5 mm [15] was integrated next to the FBG. Apart from the availability of an additional reference temperature measurement, differences in the sensitivity between fiber optic and conventional temperature sensors could be investigated in this way.

3.1 Optical backscatter reflectometry

The principle of fiber optic monitoring of temperature distribution and development in the tank ground in fire was based on the recording temperature-related changes in the Rayleigh backscattering profiles along the sensor fiber. The relative temperature measurement was ensured by a pairwise comparison of individually recorded backscattering profiles with a reference profile recorded immediately before the beginning of the test series. Moreover, the backscattering profiles from two datasets were cross-correlated in increments representing individual sensing elements. The configurable increments of typically 0.5–5 cm defined thus the spatial resolution of the distributed temperature measurement along the fiber under test. In general, the longer the increment size is, the better the temperature accuracy. In case of high-gradient temperature changes, as during the tests under fully developed fire, a trade-off must be made between the spatial resolution and temperature accuracy. In such cases, an undersized increment can lead to significant signal artifacts due to the blurring of the cross-correlation spectra. For the fire tests performed at BAM TTS, the best results could be achieved at a spatial resolution of 3.0–3.5 cm.

All distributed measurements during the fire tests were performed using a commercial unit LUNA OBR 4460. This optical frequency-domain reflectometer (OFDR) utilizes swept-wavelength interferometry [16]. This means that each measurement process is based on a wavelength sweep of the laser source used for launching light in the
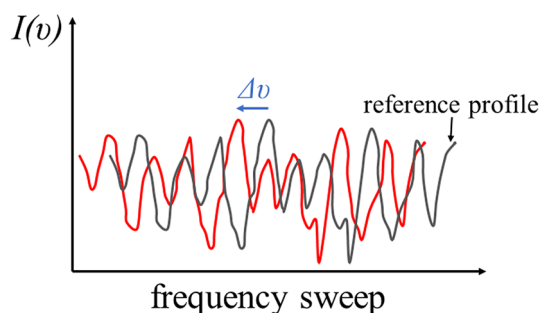
Fig. 4 Local frequency shift of recorded Rayleigh backscattering profiles caused by temperature and strain events
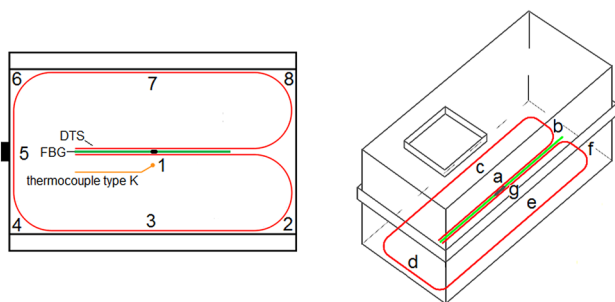
Fig. 5 Spatial position of the FOSs in the composite structure. Dimensions of the GFRP tanks: 1.50 m long, 0.90 m high and 1.03 m wide

sensing fiber. Therefore, this approach allows the detection of intensity profiles as a function of the swept laser frequency $I(v)$ along the fiber under test divided into the configurable increments mentioned above. The intensity profiles $I(v)$ varies from sensing element to sensing element, but are still stable at constant temperature and strain conditions along the sensing fiber. Such characteristic intensity fingerprints can be explained by the physical nature of the Rayleigh scattering caused by stochastic local defects and distortions as well as refractive index fluctuations along the fiber. In case of spatial changes in the external conditions affecting the sensing fiber, the characteristic intensity fingerprints are compressed or stretched leading to spatially resolved frequency shifts Δv of the intensity profiles $I(v)$ as schematically shown in Fig. 4.

The determinable spectral frequency shift Δv is linearly dependent on the temperature and strain gradients as given by the following equation:

$$\Delta v = C_T \cdot \Delta T + C_\varepsilon \cdot \Delta \varepsilon, \qquad (1)$$

where $C_T = -1.316 \frac{\text{GHz}}{\text{°C}}$ and $C_\varepsilon = -0.150 \frac{\text{GHz}}{\mu\text{m/m}}$ stand for the characteristic temperature and strain coefficient, respectively. The values of the coefficients specified above have been determined during preliminary laboratory tests on the

OBR-based sensor configuration chosen for the integration in the composite tanks.

While ensuring the mechanical decoupling of the sensing fiber using a loose-tube design of the fiber optic sensors, a pure temperature distribution along the sensing fiber can be determined.

## 3.2 Integration of fiber optic sensors

The on-site integration of FOSs in the composite tanks was carried out by a BAM team in accordance with the layout in Fig. 5 during tank-manufacturing process at VKA GmbH in Schönbrunn, Germany. The numeration 1–8 on the left side of Fig. 5 corresponds to the selected point locations in the tank bottom that are representative for the analysis of heat-related changes in composite material while taking environmental factors such as wind direction into consideration. The numeration a–g on the right side of Fig. 5 describes various sections of distributed sensors. Due to the complex geometries and possible variance in the protective impact of the applied intumescent coatings, deviations in the measuring signal in the numbered sections are expected.

After placing each GFRP tank to be tested for fire resistance on the water-cooled rack at the test site shown in Fig. 1, the embedded FOSs were connected to the measurement device placed outside the test site using fiber optic patch cables. For this purpose, the patch cables were directed out of the tanks over the water outlet opening located in the lower shells. Figure 1 shows the metal braiding hose enclosing water-cooled fiber optic patch cables. To ensure the best possible thermal insulation, the metal braiding hose was additionally wrapped with calcium silicate wool. The calcium silicate high-temperature insulation and the integrated water cooling inside the hose prevented not only directly the damage of the fiber optic patch cables, but mainly removed the high-gradient temperature changes deteriorating the measuring signals. The preliminary tests for determination of the cooling effects depending on the water flow rate revealed that a too strong water flow generates vibrations inside the hose. This in turn can lead to disturbances affecting the measuring signals. During the preliminary tests, an optimized water flow rate of 6.25 l/min was determined. Such a flow rate allows an artifact-free distributed temperature measurement with the required spatial resolution of 3 cm.

4 Fire tests

The suitability of the fire protection systems listed in Sect. 2.2 was investigated under fully developed fire as shown in Fig. 6. The fire temperature at the outside surface of the tested tanks averaged 950 °C [2]. To ensure the flame
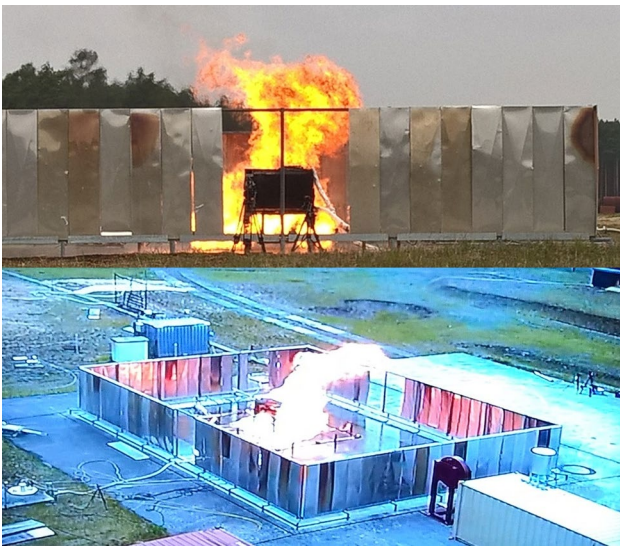
Fig. 6 GFRP tank under fully developed fire

impingement as much the same as possible, the fire tests were performed on days when wind strength was lower. The mean wind speed remained below 1.0 m/s during the most fire tests. Only the test on the tank coated with type A was performed under less favorable wind conditions with the measured wind speed averaging 1.5 m/s.

The visual inspection of the tanks after flame treatment yielded a satisfactory protective function of the two intumescent coatings A and B. On the other hand, due to the heat-related decomposition of the fire protective thermoplastic foil, shown in Fig. 7, the use of such fire protective materials cannot be recommended in this particular application. The effect of this intumescent thermoplastic foil is, therefore, not further considered below. In general, due to the strong decomposition and the associated malfunction of the thermoplastic foil, the temperature measured by the FOSs constantly exceeded the value of 120 °C after about 7 min of the start of the fire test. Such a temperature increase was

significantly faster compared to its intumescent counterparts, whose measurement results are presented in the next section.

For the sake of completeness, Fig. 8 documents the results of the visual inspection for the remaining tanks protected by the intumescent coatings. The two GFRP tanks have met the requirements of leakproofness defined by ADR.

5 Field measurements

The fire protective impact of an intumescent coating is clearly visible in Fig. 9.

By applying intumescent materials for passive fire protection, the temperature increase can be kept in the range below thermal failure of composites.

The slightly different sensor allocation in the two tanks whose measurement results are presented in Fig. 9 led to greater spatial distance between the FBG and the distributed sensor in case of the tank coated with type B. This resulted in a larger deviation in measuring signal of the FBG and the OBR-based sensor. Furthermore, also the high-temperature gradients around the first temperature peak visible in Fig. 9b can cause a superelevation of the determined OBR signal.

Generally, the FOSs provided higher temperature values compared to the thermocouple as presented in Fig. 9b. It can be an indication of their better integration in the laminate structure of the tank due to their small sizes. This assumption is reinforced by the fiber optic detection of short-term temperature drops in the 27th minute both by FBG and OBR as well as in the 46th minute by FBG. The temperature drops can point to heat-related local delamination accompanied by negative pressure and even water penetration between the affected layers of the composite structure. The two effects lead in turn to the mentioned short-term temperature drops not detected by the thermocouple. This behavior does not necessarily indicate the worse sensitivity of thermocouples compared to their fiber optic counterparts. The lack of selective detection of the temperature drops by the thermocouple can rather be explained either by its larger dimensions

Fig. 7 Heat-related decomposition of the fire protective thermoplastic foil applied on the outer tank surface
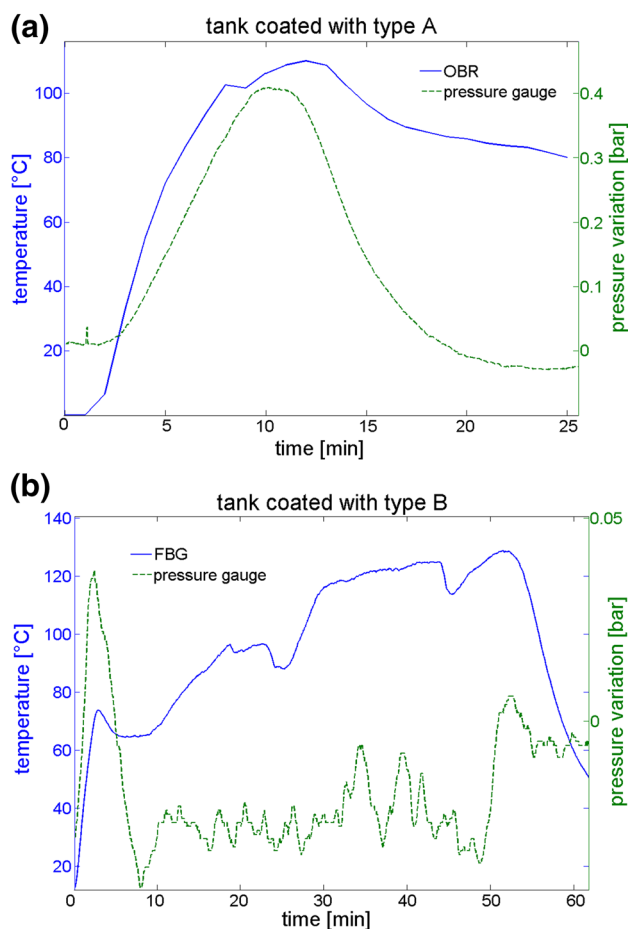

Fig. 8 Inspection after fire tests—GFRP tanks with a protective coating of type A (left) and type B (right)
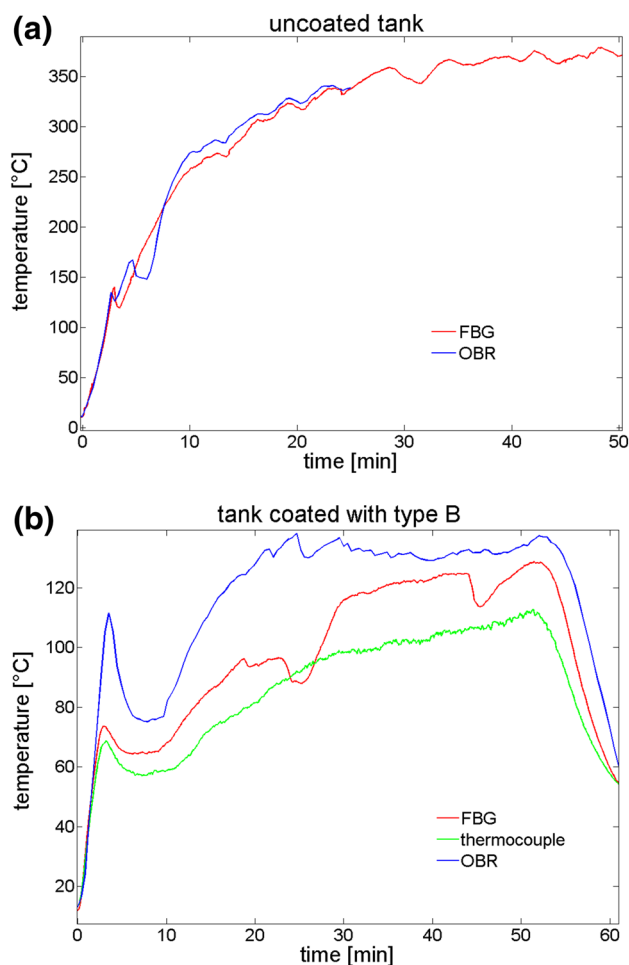
Fig. 9 Temperature development measured at the centre of the tank bottom (**a**) reference tank without additional intumescent coating—failure of the OBR measuring signal after 25 min (**b**) tank with applied intumescent coating of type B

Fig. 10 Temperature development vs. pressure inside the tank with (**a**) intumescent coating of type A and (**b**) intumescent coating of type B

impairing the composite layer structure or simply by the fact that the fiber optic and the thermocouple measurements have not been performed at the exactly same position. The larger the sizes of the embedded sensor, the more difficult the measuring quantities are to transfer from the sensor environment to the sensor itself. In addition, it is likely that the composite structure could even be pre-damaged during installation of the thermocouple providing a kind of pre-delamination phenomena. The exact causes of the sensitive differences in the case of the detected short-term temperature drops could be further investigated using the two sensor types (FOSs and thermocouples) with comparable diameters.

In contrast to the temperature drops shown in Fig. 9b and described above, also a clear temperature peak was measured after the first few minutes of the fire test. As presented in Fig. 10, the temperature peaks generally correlated in time to the overpressure peaks measured by standard pressure gauge placed inside each tank. Due to

the different overpressure levels obtained during the individual fire tests, differing reasons for the observed reduction in pressure can be supposed in the two cases presented in Fig. 10. In the case (a), a buckle of the sealing system of the tank lid can be assumed. Since the sealing action was diminished in advance of the remaining fire tests, the reasons for the detected reduction in pressure cannot be clearly identified for the case (b). However, the fact is that from a physical point of view, the reduction in pressure can result in the temperature decrease. Furthermore, the assumption of different reasons for the pressure decrease is further reinforced by measurements presented in Fig. 11.

The upper diagram in Fig. 11 (case a) proves that the distinctive temperature peak was observed only at the central position 1, whereas the lower diagram (case b) reflects the independence of the measurement point position for the occurrence of the temperature peak.

The results of the distributed measurements presented in Fig. 12 provide spatially resolved information about the temperature development over time in the tank bottom along the whole sensing fiber. The diagram in Fig. 12 can thereby
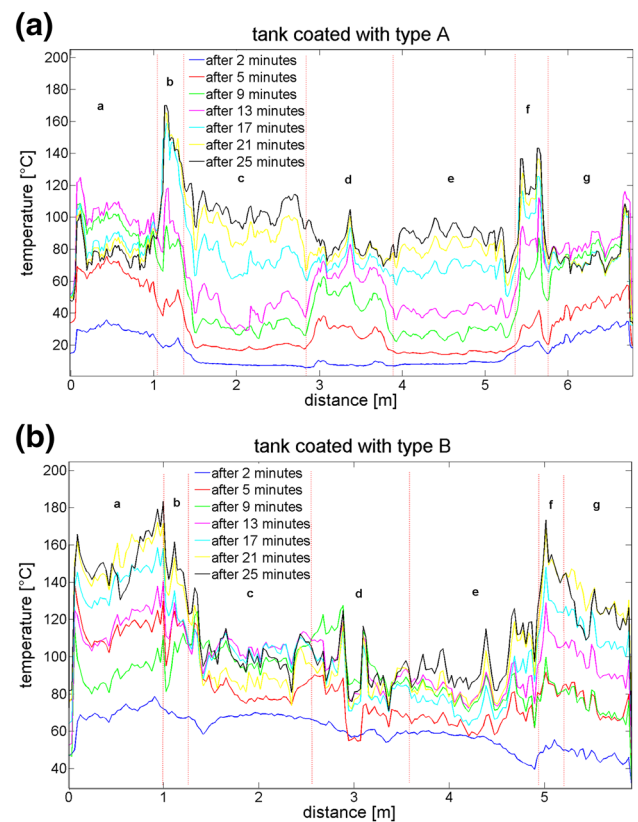
(a)

(b)
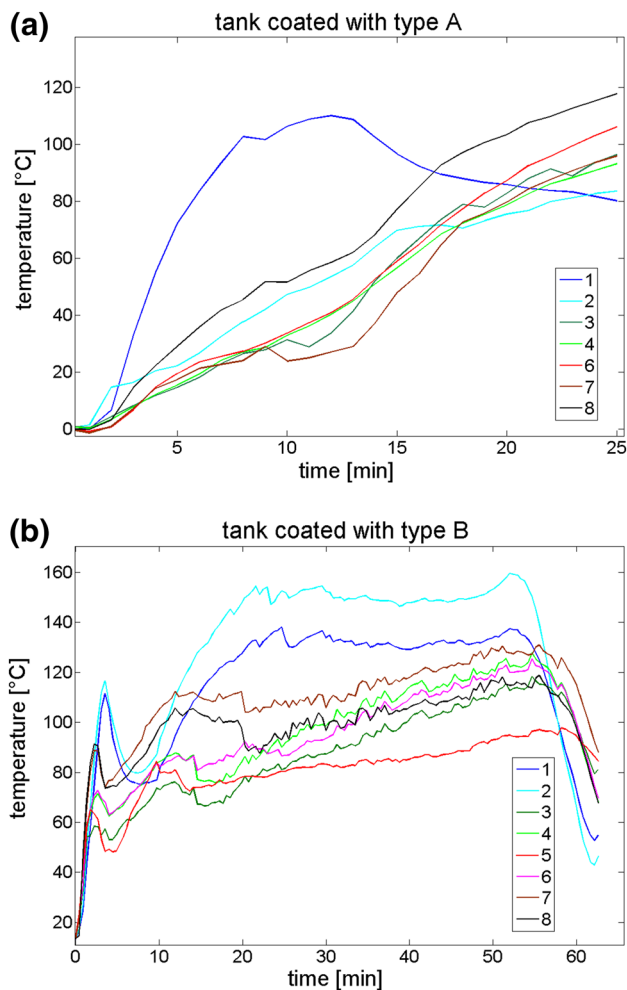
Fig. 11 Position-related temperature differences in the tank bottom coated with (**a**) type A and (**b**) type B measured by OBR

(a)

(b)

Fig. 12 Temporal development of temperature distribution in the tank bottom coated with (**a**) type A and (**b**) type B

deliver a response to the problem of possible shape-related differences in the protective effect of intumescent coatings presented for the coating of type A and B.

In consequence of the complex shape of the tanks, there are three groups of comparable sensing fiber sections shown in the allocation plan in Fig. 5:

- centrally located sections: a and g
- sections placed on supports: c and e
- unsupported sections: b, f and d.

The measurement data presented in Fig. 12a prove similar temperature increase with time in sections c and e. The temperature development in sections a and g of the tank coated with type A provides evidence for the unexpected temperature decrease initiated in the 13th minute after the start of the fire test. This behavior can be explained by the viscous softening of the matrix at the area of the highest weight-related deformation causing water ingress with its cooling effect.

In contrast to the section-wise similarity of temperature development described above, an important discrepancy in the temperature behavior in sections b and f compared to d can be identified. Furthermore, the signal increase observed in b and f can be explained by friction-related strain cross-sensitivity in the both sections caused by critical bending of the tube including the sensing fiber. As presented in Fig. 12a, the temperature distribution recorded 25 min after the beginning of the fire test on the tank coated with type A shows the maximum temperature value in the section b exceeding the remaining temperature values by about 70 °C. Under the assumption of a certain behavioral comparability of the temperature development in the sections b, f and d, such a signal enhancement in the range of 70 °C cannot correspond to a real temperature increase. It can, therefore, be considered that the excessive spectral frequency shifts measured by the OBR system are caused both by the fire-related temperature gradients and by an additional friction-related strain increase. Applying the knowledge about the temperature and strain coefficients of the OBR-based sensor determined during the preliminary laboratory tests, the temperature change of 1 °C can correspondingly be treated as a strain change of 8.776 μm/m. In this way, the unexpected signal peak in the section b thus represents the friction-related strain increase

up to 600 μm/m and not the 70 °C rise in temperature shown in Fig. 12a.

By choosing stainless steel tubes with an inner diameter of 0.45 mm instead of 0.20 mm, the friction-related strain cross-sensitivity has been suppressed in the subsequent fire tests as clearly presented in Fig. 12b. Here, the use of the new design of temperature sensors based on the larger diameter of the stainless steel tubes used in the tank coated with type B resulted in a significant decrease of the measuring signals recorded in the sections b and f.

6 Conclusion

The use of FOSs has proven to be a promising solution for monitoring of heat-related changes in the composite layer structures. The key application-related advantage of FOSs lies in the distributed type of measurements providing important data about the local failure of the intumescent coatings along the whole sensing fiber without spatial gaps. These findings might be of use to the fire-retardant tank manufacturing to improve and optimize the performance of the fire-resistant coatings. Other important information could be obtained from supplementary measurements to be performed after the fire-tested tanks have cooled down to the ambient temperature. Such additional investigation of possible residual strains or temperature offsets has not been conducted here.

Regarding the prevention of pre-damage of the layer structure in the form of air inclusion or resin pocket all the embedded sensors should have small diameters. This provides better integration in the monitored structure, simultaneously increasing the measurement sensitivity. Thanks to such an application-related improvement of the sensor sizes, also electrical point sensors in the form of thermocouples or resistance temperature detectors (RTDs) can provide important information about punctual material changes.

In case of the distributed monitoring system based on OBR, due to the adjustment of the water flow rate cooling the fiber optic cable supply lines, the blurring of the cross-correlation spectra could be avoided. In this way, a high spatial resolution of 3 cm has been realized without detrimental signal distortion.

References

1. Mouritz AP, Gibson AG (2007) Fire properties of polymer composite materials, vol 143. Springer Science & Business Media, New York. https://doi.org/10.1007/978-1-4020-5356-6
2. Pötzsch S, Timme S, Sklorz C, Skoczowsky D, Otremba F, Krüger S (2017) Fire protection systems for tanks made of GFRP. International mechanical engineering congress and exposition. Am Soc Mech Eng. https://doi.org/10.1115/IMECE2017-70381
3. Hörold A, Schartel B, Trappe V, Gettwert V, Korzen M (2015) Protecting the structural integrity of composites in fire: intumescent coatings in the intermediate scale. J Reinf Plast Compos 34(24):2029–2044. https://doi.org/10.1177/0731684415609791
4. Gibson AG, Feih S, Mouritz AP (2011) Developments in characterising the structural behaviour of composites in fire. Composite materials. Springer, London, pp 187–218
5. Birman V, Kardomateas GA, Simitses GJ, Li R (2006) Response of a sandwich panel subject to fire or elevated temperature on one of the surfaces. Compos Part A Appl Sci Manuf 37(7):981–988. https://doi.org/10.1016/j.compositesa.2005.03.014
6. Timme S, Trappe V, Korzen M, Schartel B (2017) Fire stability of carbon fiber reinforced polymer shells on the intermediate-scale. Compos Struct 178:320–329. https://doi.org/10.1016/j.compstruct.2017.07.025
7. Duquesne S, Magnet S, Jama C, Delobel R (2004) Intumescent paints: fire protective coatings for metallic substrates. Surf Coat Technol 180:302–307. https://doi.org/10.1016/j.surfcoat.2003.10.075
8. Jimenez M, Duquesne S, Bourbigot S (2006) Intumescent fire protective coating: toward a better understanding of their mechanism of action. Thermochim Acta 449(1–2):16–26. https://doi.org/10.1016/j.tca.2006.07.008
9. Samiec D (2012) Distributed fibre-optic temperature and strain measurement with extremely high spatial resolution. Photon Int 6:10–13
10. Hill KO, Meltz G (1997) Fiber Bragg grating technology fundamentals and overview. J Lightwave Technol 15(8):1263–1276. https://doi.org/10.1109/50.618320
11. De Oliveira R, Ramos CA, Marques AT (2008) Health monitoring of composite structures by embedded FBG and interferometric Fabry–Pérot sensors. Comput Struct 86(3–5):340–346. https://doi.org/10.1016/j.compstruc.2007.01.040
12. Vikas SD, Grover A (2015) Fabrication and applications of fiber Bragg grating—a review. Adv Eng Technol Appl 4(2):15–25
13. United Nations (2006) European Agreement concerning the international carriage of dangerous goods by road (ADR). In: ADR 2007, United Nations Publications
14. Ridder K, Holzhäuser J (2017) ADR 2017. ecomed-Storck GmbH, Hamburg
15. Artmann N, Vonbank R, Jensen RL (2008) Temperature measurements using type K thermocouples and the Fluke Helios Plus 2287A data logger. In: Technical report. Aalborg University
16. Kreger ST, Gifford DK, Froggatt ME, Soller BJ, Wolfe MS (2006) High resolution distributed strain or temperature measurements in single-and multi-mode fiber using swept-wavelength interferometry. Opt Fiber Sens. https://doi.org/10.1364/OFS.2006.ThE42